An Experimental Investigation of Turbulent Slot Injection at Mach 6

K. PARTHASARATHY* AND V. ZAKKAY†
New York University, Bronx, N. Y.

The use of film cooling for protecting a surface exposed to high temperature air at hypersonic speeds is investigated experimentally. The tests were conducted in a Mach 6 contoured axisymmetric nozzle with a streamlined centerbody. The Reynolds number in the test section was in the range of 1-3.6 $\times$ 10^6/in.; and a wall to freestream temperature ratio of 0.635. Heat-transfer distributions downstream of the slot were obtained for various mass flow rates and the effect of injection on the velocity, temperature and Mach number profiles was studied. Correlations for the cooling lengths with the blowing rate parameters $\lambda = \rho_J U_J/\rho_e U_e$ for the various coolants—air, helium, hydrogen, and argon were obtained. Correlations for the heat-transfer rates in the form $(1 - q/q_{0.i})$ and for the effectiveness $[\epsilon = (T_{aw} - T_{0\infty})/(T_{0J} - T_{0\infty})]$ of the adiabatic wall temperatures were obtained as a function of λ and x/S (distance from the slot/slot width) for each of the injected coolant gases. The adiabatic wall temperatures are not a basic result of the measurements, but have been inferred from the heat transfer measured, using a local flat plate equation for the same wall temperature. Skin-friction coefficients were also obtained from the measured profiles. Finally the results of this study are compared with available results in the literature.

Nomenclature

$c_{w.m}$ = specific heat of wall material
C_f = compressible skin-friction coefficient
c_p = constant pressure specific heat
$d_{w.m}$ = thickness of wall material
h = enthalpy
M = Mach number
P = local static pressure
Pr = Prandtl number
q = local heat-transfer rate at the wall with injection
$q_{0.i}$ = local heat-transfer rate at the wall without injection
Re = Reynolds number = $U_e x/\nu_e$
S = slot width
St = Stanton number
T = static temperature
T_{aw} = adiabatic wall temperature
t = time
U = velocity in the streamwise direction
x = streamwise coordinate
y = coordinate normal to body surface
γ = ratio of specific heats
ϵ = effectiveness of cooling $(T_{aw} - T_{0\infty})/(T_{0J} - T_{0\infty})$
λ = ratio of mass flow throughout the slot per unit area to the mass flow of the mainstream per unit area $(\rho_J U_J)/(\rho_\infty U_\infty)$
ρ = density
$\rho_{w.m}$ = density of the material of the model
δ = thickness of boundary layer
δ^* = displacement thickness

Subscripts

e = edge of boundary layer
∞ = freestream conditions
w = conditions at the wall
J = jet conditions
0 = stagnation conditions
$C.L$ = cooling length
$w.m$ = wall material
$0.i$ = no injection

I. Introduction

IN general, film cooling involves the introduction of a coolant fluid through discrete slots positioned along the surface to be cooled, to insulate thermally the surface from the hot stream.

A set of exhaustive tests was carried out by NASA[1] on improving gas-turbine-blade cooling. The tests were entirely empirical and specialized. Along similar lines were the tests of Kueppers as reviewed by Meyer.[2]

Film cooling studies first were performed by Wieghardt.[3] Later investigations include those by Seban,[4] Papell and Trout,[5] Hartnett, Birkebak and Eckert[6] and Chin, Skirvin, Hayes, and Burggraf.[7] Eckert and Birkebak[8] compare many of these earlier studies and also provide the results of additional experiments. These experimental investigations employed low-speed subsonic flow in both primary and secondary streams. The freestream velocity was approximately uniform as is the case in the present investigation. A study of film cooling in a supersonic flow about a hemisphere was presented by Dannenberg.[9]

Wieghardt's study of the effects of hot air injection from a discrete slot into a turbulent boundary layer consisted of the measurement of the adiabatic wall temperature distribution downstream from the point of injection, and the subsequent development of the velocity and temperature boundary-layer profiles. In Wieghardt's investigations, the secondary or injected air was introduced in a direction almost parallel to the mainstream.

Seban et al.[10,11] performed experiments for tangentially injected air with a slightly different slot configuration than Wieghardt. Their reported dimensionless adiabatic wall temperature distribution, the so-called effectiveness, is somewhat at variance with that of Wieghardt. Chin et al.[12] using a slot configuration similar to Seban,[4] have obtained values of the dimensionless adiabatic wall temperature for various injection rates. The correlation achieved for these data give higher results than the data of Seban and Wieghardt.

Received February 21, 1969; revision received December 1, 1969. This research was supported by the Aerospace Research Laboratories, Office of Aerospace Research, U.S. Air Force, under Contract F33615-68-C-1184, "Boundary Layer Characteristics for Hypersonic Flow," and forms part of the Ph.D. thesis of K. Parthasarathy at New York University.

* Assistant Research Scientist, Department of Aeronautics and Astronautics.

† Professor, Department of Aeronautics and Astronautics. Associate Fellow AIAA.

The later results for tangential injection are reported by Papell et al. and are concerned with large temperature differences between the freestream and the injected air. The slot configuration is similar to that of Seban[4] and the effectiveness is in fair agreement with the earlier study. Several different correlations are proposed for the effectiveness for various ranges of mass injection. Goldstein, Eckert, Tsou, and Haji-Sheikh[13] investigated the effects of air and helium injection through a rearward facing slot in a supersonic (Mach 3) mainstream for various blowing rates along a flat plate. The total temperature of the mainstream was approximately room temperature and the injectant temperature was between 418° and 655°R. (The results could be interpreted as film heating rather than film cooling.) The results were correlated on the basis of adiabatic wall temperature measurements. They obtained different correlations for the cooling length and the effectiveness parameter for $\lambda < 0.12$ and $\lambda > 0.12$. The effectiveness ϵ was based on recovery temperature for no injection rather than on stagnation temperature.

Samuel and Joubert[14] conducted investigations on an adiabatic flat plate in zero pressure gradient downstream of a tangential injection slot. The experimental conditions were a hot subsonic mainstream and cold secondary injection. Results were presented for wall temperature distributions at varying ratios of injected to mainstream mass flow. They obtained different correlations for the effectiveness ϵ for differing slot widths and blowing rates but they concluded that the results could be correlated as $\epsilon = \text{fn}(x/S)^{-0.5}$ for $\lambda = 0.88$. The discrepancy could be due to the prolonged secondary flow-absorption zone examined in their work.

In the present work, the effectiveness of slot cooling is experimentally investigated. The mainstream Mach number is designed to be 6.0. The coolant gas is injected at sonic velocity. Helium, hydrogen, argon, and air at room temperature are employed as coolants. The effect of slot injection in a direction downstream of the mainstream is studied. Heat-transfer rates are measured using thin-wall techniques. Correlations for cooling lengths and effectiveness of adiabatic wall temperatures are investigated. The absence of adequate data on film cooling at high Reynolds numbers and large blowing rates prompted these investigations. The boundary layer profiles and the computation of skin friction from the measured profiles are investigated.

II. Experimental Apparatus

A. Wind Tunnel

The New York University (NYU) Aerospace Laboratory High Reynolds Number facility is a blowdown type wind tunnel. It has a regenerative type heater and a Mach 6 contoured axisymmetric nozzle with a 12-in.-diam test section. The regenerative heater is designed to maintain a constant output temperature during a typical wind-tunnel run time of 30 sec. The wind-tunnel and heater design are described in detail in Ref. 15. The stagnation temperature for the present experiments ranged from 720° to 900°R and the stagnation pressure from 400 to 2000 psia. The corresponding Reynolds number range at Mach 6 was from 1.2×10^7 to 4.1×10^7/ft.

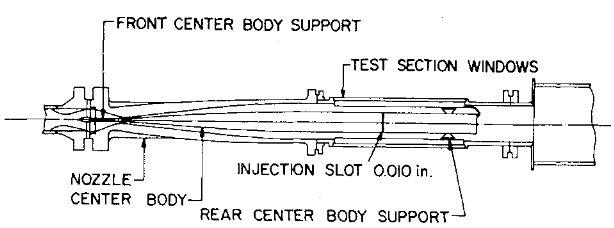

Fig. 1 Details of film cooling model with centerbody support and test section.

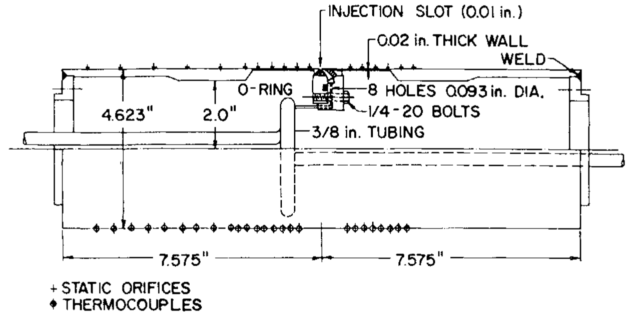

Fig. 2 Details of model construction for upstream and downstream injection.

B. Model

The model, shown schematically in Figs. 1 and 2, is a streamlined axisymmetric centerbody 72.5 in. long and passing through the throat of the nozzle. The slot is located 15 in. downstream of the Mach cone and therefore uniform flow is established well ahead of the injection region. A 20-in.-long cylindrical attachment equipped with instruments was added downstream of the 15-in. cylindrical section for making measurements far downstream of the injection station. The injection slot was located 60 in. from the nozzle throat. The slot height was 0.01 in. compared with 0.85-in. boundary-layer thickness, at nominal test conditions.

C. Instrumentation

The model was instrumented with static pressure taps and locally thin-skinned type heat-transfer gages (see Fig. 2). Pitot pressure, static pressure, and total temperature profiles were obtained by traversing the boundary layer from the model wall to the external flow with a forked combination triple probe. The probe was moved in the normal direction with an automatic traversing mechanism, and could also move in the flow direction. The details of the probe construction, instrumentation, and recording equipment are given in Ref. 25.

The main difficulty in the present measurements was encountered when the probe approached the sonic line of the boundary layer. As explained by Bradfield,[16] a complex interaction phenomenon occurs between the probe shock and the subsonic region of the boundary layer. This interaction gives rise to erroneous measurements in the vicinity of the wall. It is estimated that based on the size of the probe used in the present experiments that the measurements are in error at heights below 0.03 in. from the wall.

III. Data Reduction

A. Heat Transfer

To evaluate the heat transfer the transient thin-wall technique is used. The heat transfer is determined from the slope of the temperature-time record of the temperature of the thermocouples on the model. The heat transfer is given by the relation (assuming one-dimensional heat transfer)

$$q = \rho_{w.m} c_{w.m} d_{w.m} (dT/dt)_{t=0} \tag{1}$$

In order to eliminate any similar variation if any, in the measurements, the heat-transfer rates at each thermocouple position were normalized with respect to the heat transfer rates without injection. Therefore, the efficiency of each injection test was indicated by the ratio $q/q_{0.i}$ at each gage location.

B. Adiabatic Wall Temperature

The adiabatic wall temperatures have been calculated by the Flat Plate Reference Enthalpy Method (FPRE);[17]

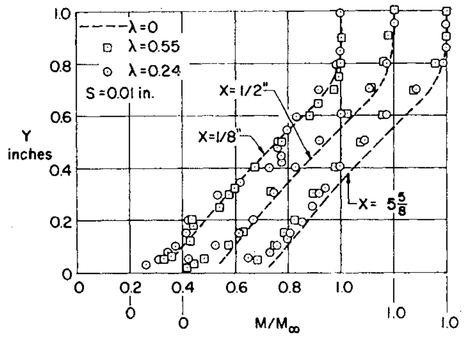

Fig. 3 Mach number profiles for downstream injection.

Zakkay and Callahan[18] have shown that heat transfer rates for turbulent boundary layers even in mild adverse pressure gradients are predicted with reasonable accuracy by the aforementioned method.

The FPRE method assumes that boundary-layer heat-transfer phenomena are determined by local flow conditions and are independent of gradients in the stream direction. It assumes that the fluid properties are constant across the boundary layer and are evaluated at the reference enthalpy defined by

$$h^* = 0.5h_w + 0.22Pr^{1/3}h_{0\infty}(0.5 - 0.22Pr^{1/3}) \tag{2}$$

Based on experimental results the FPRE assumes that

$$\text{Stanton No.} = St = 0.0296/[(Re^*)^{0.2}(Pr)^{2/3}] \tag{3}$$

where * denotes quantities at the reference enthalpy.

C. Profile Data

The static pressure and the stagnation pressure (behind the normal shock wave) in the boundary layer are measured to determine the Mach number distribution in the boundary layer.

The velocity profiles (U/U_e) are obtained from the Mach number and total temperature profiles. The profiles of density ($\rho/\rho_e = \bar{\rho}$) are obtained from the values of static pressure (P_{stat}), total temperature (T_0), and the computed values of the Mach number. The computed density profiles along with the velocity profiles are used to determine the skin-friction coefficients.

Many investigators, in the past have tried to use transformation theory and available incompressible layers in compressible flow. Recently, Baronti and Libby[19] have carried out a point-by-point mapping of compressible, turbulent boundary layer flows into constant density flows as suggested by Coles[20] transformation theory. The variety of compressible constant pressure velocity profiles considered were all correlated by the law of the wall.[19] The method of Ref. 19 was used to correlate the experimental velocity profiles and hence obtain skin friction.

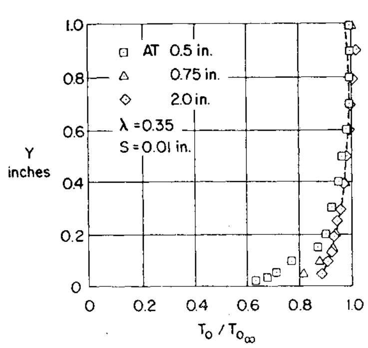

Fig. 4 Temperature profiles for downstream injection.

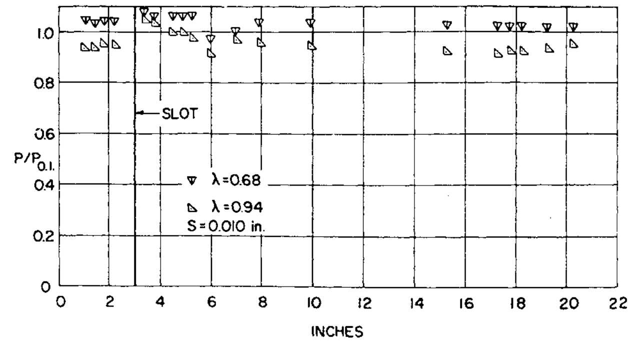

Fig. 5 Wall static pressure distribution for downstream injection.

IV. Results and Discussion

The experimental investigations include two areas of work. The wall heat transfer distributions provide a picture of the effectiveness of the secondary injection. The boundary-layer profile work is useful in providing a picture of the secondary flow absorption zone.

The experimental conditions are as follows: mainstream Mach number = 6, mainstream temperature = 750°–850° R, mass flow ratio λ = 0–3.2, x/S = 40–2000. Profiles of U/U_∞, M/M_∞ and $T_0/T_{0\infty}$ vs y are shown in Figs. 3 and 4.

A. Mach Number and Velocity Profiles

For downstream injection, there is a mixing zone near the slot for mass flow ratios of $\lambda = 0.55$ and 0.24. For higher mass flow ratios (close to 1.0) the region of mixing is narrower probably due to the less rapid rate of mixing. The effect of the secondary flow on the mainstream is to increase the mainstream momentum throughout the secondary flow absorption zone. Downstream of the slot, the inner layer has merged with the outer region of flow, and farther downstream the profiles have the character of a fully developed turbulent boundary layer with a larger effective thickness (Fig. 3). The boundary layer is fully recovered to the no injection profile at approximately 18 in. from the injection slot (x/S = 1800) at the higher value of λ.

B. Temperature Profiles

The total temperature profiles obtained at various locations on the model show the characteristics of a typically hypersonic profile (Fig. 4).

In the case of downstream injection, the cooling effect is more localized (near the wall) and the drop in temperature in the profile is much larger showing up as a sudden jump. Far downstream the typical no injection hypersonic turbulent boundary-layer temperature profile is regained.

C. Static Pressure Distributions

The static pressures measured on the wall, both up and downstream of the slot, are shown in Fig. 5 for various blowing rates. It is clearly observed that static pressure increases slightly, immediately downstream of the slot due to the formation of the compression region and is recovered to the original pressure rapidly. The increase in static pressure observed at the Reynolds number of the tests conducted was so small that it would possibly affect the heat-transfer results to an extent smaller than the accuracy of the measurement of the heat transfer. Consequently, no corrections have been applied to the measured heat-transfer results at the Reynolds number for the majority of the tests run.

D. Heat-Transfer Distributions

Heat-transfer rates have been plotted as $q/q_{0.i}$ (q = heat transfer with injection; $q_{0.i}$ = heat transfer with no injec-

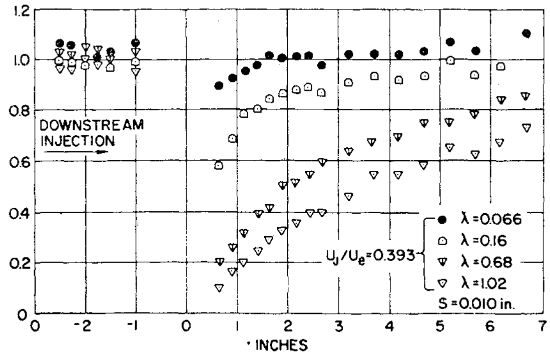

Fig. 6 Heat-transfer distributions for downstream air injection.

tion) against x/S (x = distance downstream of the slot; S = slot width).

It was observed that for constant λ, the heat-transfer distributions are almost identical at varying Reynolds numbers (in the range tested). Hence, it was decided to correlate the results with λ. The heat-transfer rates measured for zero injection were within 10% of the values calculated using Eq. (3).

The values of $q_{0.i}$ measured also agreed very well with the values of the heat transfer measured in Ref. 15 (no shock generator) which used the same model as used here. The heat-transfer rates decrease in the beginning since the wall effectively "sees" only the coolant gas and a region dominated by the coolant is present very close to the slot. The hot mainstream gas mixes with the coolant downstream and thus, the increase in heat-transfer rates. The cooling length (the length downstream of the slot where the adiabatic wall temperature is equal to the injectant stagnation temperature), and the recovery of the heat transfer depends on the mixing phenomenon, the blowing rate and the specific heat of the coolant. The heat-transfer rates are reduced to values very close to zero depending on the blowing parameter, and increase gradually downstream to the no injection values. A typical heat-transfer distribution is shown in Fig. 6.

Tests were conducted with different coolant gases—argon, helium, hydrogen, and air. It was found that for each coolant gas, the heat transfer distributions could be correlated onto a single curve as shown in Fig. 7. Such a plot was obtained using $(1 - q/q_{0.i})$ for the y axis and $x/S\lambda^{0.8}$ for the x axis. For each gas a correlation curve was obtained. The results of the correlation were as follows:

$$1 - \frac{q}{q_{0.i}} = 900\left(\frac{x}{S\lambda^{0.8}}\right)^{-0.97} \text{ for hydrogen injection for } \frac{x}{S\lambda^{0.8}} \geq 1100 \quad (4)$$

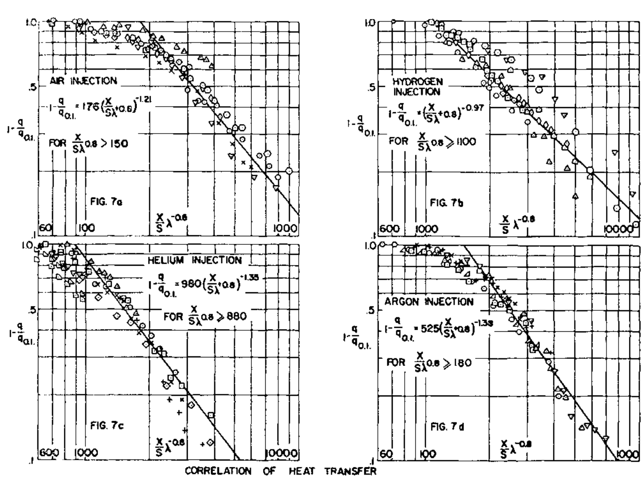

Fig. 7 Correlations for heat transfer.

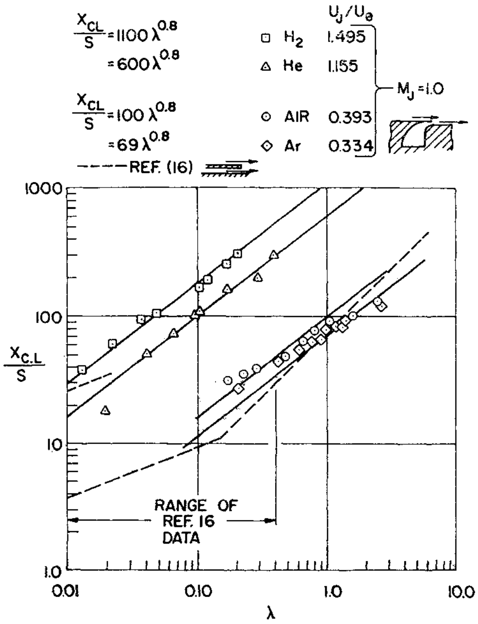

Fig. 8 Correlations for cooling lengths.

$$1 - \frac{q}{q_{0.i}} = 5980\left(\frac{x}{S\lambda^{0.8}}\right)^{-1.28} \text{ for helium injection for } \frac{x}{S\lambda^{0.8}} \geq 880 \quad (5)$$

$$1 - \frac{q}{q_{0.i}} = 525\left(\frac{x}{S\lambda^{0.8}}\right)^{-1.21} \text{ for air injection for } \frac{x}{S\lambda^{0.8}} \geq 180 \quad (6)$$

$$1 - \frac{q}{q_{0.i}} = 1010\left(\frac{x}{S\lambda^{0.8}}\right)^{-1.38} \text{ for argon injection for } \frac{x}{S\lambda^{0.8}} \geq 150 \quad (7)$$

The correlations for the effectiveness of film cooling are shown in Fig. 9. The correlations show plots of the effectiveness ϵ vs. $x/S\lambda^{0.8}$. A plot of this form was found to collapse all the curves for different λ's on to a single line. The effectiveness was defined on the basis of freestream stagnation temperature.

The correlations for the cooling lengths corresponding to point A (Fig. 9) are shown in Fig. 8. The results could be correlated according to the following equations:

$$x_{C.L}/S = 1100\lambda^{0.8} \text{ for hydrogen injection} \quad (M_J = 1.0;\ U_J/U_e = 1.495) \quad (8)$$

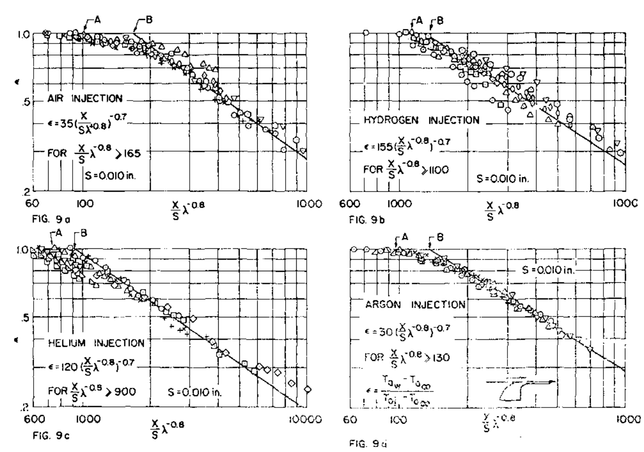

Fig. 9 Correlations of film cooling effectiveness.

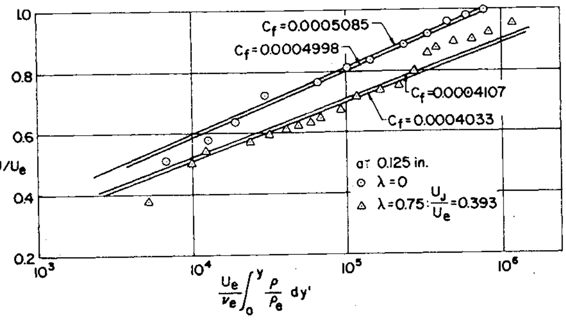

Fig. 10 Determination of skin friction.

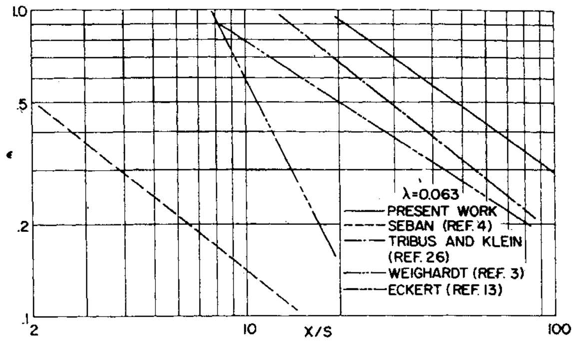

Fig. 11 Film cooling effectiveness as predicted by subsonic and supersonic correlations (S = 0.01 in.).

$$x_{C.L}/S = 600\lambda^{0.8} \text{ for helium injection} \quad (M_J = 1.0;\ U_J/U_e = 1.155) \quad (9)$$

$$x_{C.L}/S = 100\lambda^{0.8} \text{ for air injection} \quad (M_J = 1.0;\ U_J/U_e = 0.393) \quad (10)$$

$$x_{C.L}/S = 69\lambda^{0.8} \text{ for argon injection} \quad (M_J = 1.0;\ U_J/U_e = 0.334) \quad (11)$$

Looking at Fig. 9, it is seen that there is a region between points A and B in which ϵ decreases from 1.0 to 0.9. Beyond the point B the correlations for the results lie on a line as shown. Thus the effectiveness for the adiabatic wall temperatures could be correlated according to the following equations:

$$\epsilon = 155(x/S\lambda^{0.8})^{-0.7} \text{ for hydrogen injection for } x/S\lambda^{0.8} \geq 1100 \quad (12)$$

$$\epsilon = 120(x/S\lambda^{0.8})^{-0.7} \text{ for helium injection for } x/S\lambda^{0.8} \geq 900 \quad (13)$$

$$\epsilon = 35(x/S\lambda^{0.8})^{-0.7} \text{ for air injection for } x/S\lambda^{0.8} \geq 165 \quad (14)$$

$$\epsilon = 30(x/S\lambda^{0.8})^{-0.7} \text{ for argon injection for } x/S\lambda^{0.8} \geq 130 \quad (15)$$

The differences in the constants of the correlating equations are related to the different heat capacities of the injectant gases.

E. Skin Friction

The skin-friction coefficients for the measured velocity profiles have been computed using the method of Libby and Baronti as described earlier. The reductions in skin-friction coefficients obtained are a maximum near the slot and increase gradually to the no injection value downstream. The reductions in local skin friction measured were up to 40% of the no injection values.

The "law of the wall" profile is seen clearly from the experimental measurements in the transformed plane. The measured values of the skin friction derived for the undisturbed velocity profile corresponds closely to the predicted values of Spalding and Chi.[15,21] The decrease in the friction coefficients also are found to be consistent with the measured heat transfer distributions. The determination of skin friction from the velocity profiles is shown in Fig. 10.

F. Comparison with Previous Results

The correlations for the effectiveness of film cooling for supersonic and subsonic mainstream are shown in Fig. 11. Large variations are observed in the correlations between the various results. The differences are largely due to the different ratios of the boundary layer thickness to the slot width (δ/S) and the freestream Mach number used in the various investigations.

Seban[22] investigated the effects of initial boundary layer thickness on the effectiveness. He conducted experiments varying the slot width from 0.063 in. to 0.25 in. with relative injection rates $0.25 < \lambda < 0.8$, producing changes in δ/S from $0.6/0.25 = 2.4$, to $0.60/0.063 \sim 10$. He found with the above variables, that the effect on the correlations were small with a thin boundary layer ($\delta/S \approx 2.4$). The reduction in effectiveness was much larger for a larger $\delta/S \approx 10$, being about 20% at 300 slot widths downstream.

Chin[12] has presented results with a larger initial boundary layer thickness and slot width of 0.11 in. ($\delta/S = 0.8/0.11 \approx 7$). The initial boundary-layer thickness was varied, and in those results there were greater changes in the density ratio. Chin, using greater boundary-layer thickness, obtained larger values of the effectiveness compared to those of Seban.

The local influence of initial boundary-layer thickness is complicated, and is not considered in this paper. At intermediate distances the effectiveness is increased and the final reduction is obtained by a more rapid decay at large distances downstream, and would result in a larger initial cooling length.

In the present investigations, the ratio of the initial boundary-layer thickness to slot width is much larger ($\delta/S \approx 90$) than has been previously reported. The large thickness of the boundary layer as compared to the slot width results in a much lower rate of mixing between the two streams and hence results in the larger initial cooling lengths. Also, there is a considerable difference between subsonic and supersonic mainflow and this contributes also to the differences in the correlations.

V. Conclusions

An experimental investigation of the film cooling of hypersonic turbulent boundary layers on an axisymmetric model has been carried out at a Mach number of 6.0, Reynolds numbers of up to 3.6×10^6/in., and a wall temperature ratio of $T_w/T_{0\infty} = 0.635$ for the values of blowing rate parameter $\lambda = 0$ to 3.2 using gaseous helium, hydrogen, argon, and air at room temperature as injectants. Based on the experimental results, the following conclusions have been reached.

1) For downstream injection, there are three distinct regions. Close to the slot there is a region where the adiabatic wall temperature is equal to the coolant stagnation temperature. The edge of this region (point A) corresponds to the cooling length and could be correlated as a function of the blowing rate λ. The cooling lengths corresponding to point A ($\epsilon = 1.0$) have been found to correlate according to Eqs. (8–11).

2) The second region corresponds to points downstream of the point A. In this transition region, the mixing exhibits a nonsimilar nature. No correlations have been obtained in this region. The region occurs between $\epsilon = 1.0$ and 0.9. For $\epsilon = 0.9$, it is seen that the protection could be increased

to twice the length predicted by Eqs. (8–11) which corresponds to $\epsilon = 1.0$.

Farther downstream, the effectiveness decays in a power-law form (linear in a log-log plot). The effectiveness can be correlated according to Eqs. (12–15). The difference in the numerical constants appearing in the equations are evidently due to the differences in heat capacities of the injectants. The equations could be approximately correlated by a unified equation if each of them is multiplied by $(C_p)_i/(C_p)_{air}$ where $(C_p)_i$ is the specific heat of the gas injected.

3) The variation of the static pressure on the wall indicated a variation of about 8%. The change in heat transfer due to the static pressure variation is correspondingly smaller.

4) The measured values of the heat transfer distributions for each injectant have been found to correlate according to the Eqs. (4–7).

5) The measured boundary-layer stagnation temperature profiles indicate good agreement with the Crocco temperature distribution.

6) Correlations of experimental velocity profiles by the method of Baronti and Libby[19] indicates that for the velocity profiles measured, a reasonably defined logarithmic portion can be identified.

7) Values of the compressible skin friction estimated by the method of Baronti and Libby indicates a reduction in local skin friction of up to 40% (up to $\epsilon = 1$) and an integrated reduction of up to 12% over the entire region (from the slot up to the point of $q/q_{\text{zero injection}} = 1$).

8) The fully developed turbulent boundary layer is recovered within 20 boundary layer thickness or about 1800 slot widths downstream for the blowing rate corresponding to $\lambda = 2.0$. Consequently, a developed boundary layer of larger thickness and higher equivalent Reynolds number but "similar" in character results. The thickening of the boundary layer, about 10%, causes the reduction in skin friction and a consequent reduction in heat transfer.

9) The value of "n" in the power law $[U/U_\infty = (y/\delta)^{1/n}]$ for the profiles measured was found to be 7.5 for the fully developed boundary layer at the Reynolds number of the tests.

10) A comparison between the film cooling effectiveness with supersonic and subsonic mainflow is shown in Fig. 11. The major difference between the present results and previous subsonic and supersonic results is a) the much higher Mach number which tends to increase the effectiveness of slot cooling; b) the differences in the ratio of the boundary-layer thickness to the slot width; c) the very large Reynolds number used in the present work.

11) For δ/S very large, the correlation parameter is a function of the ratio of the mass flow in the boundary layer to that of the injectant gas.

It is suggested that further tests in slot cooling be conducted varying a) the slot width; b) freestream Reynolds number, c) the stagnation temperature ratios of the coolant and mainstream, d) the ratio of the wall to freestream stagnation temperature $(T_w/T_{0\infty})$. These tests should be done exhaustively for the downstream injection case, to understand the phenomenon. Parts 1 and 2 are presently under study at the NYU Aerospace Laboratory.

References

[1] Hatch, J. E. and Papell, S. S., "Use of a Theoretical Flow Model to Correlate Data for Film Cooling or Heating an Adiabatic Wall by Tangential Injection of Gases of Different Fluid Properties," TN D-130, Nov. 1959, NASA.

[2] Meyer, R. E., "The Boundary Layer Cooling of a Flat Plate," R and M 2420, 1951, Aeronautical Research Council.

[3] Wieghardt, K., "Uber das Ausblasen von Warmluft für Enteiser," Research Report 1900, 1943, Zentrale für Wissenschaftliches Berichtwessen; also AAF Translation, Research Report F-TS-919-RE Aug. 1946, Wright Field.

[4] Seban, R. A., "Heat Transfer and Effectiveness for a Turbulent Boundary Layer with Tangential Fluid Injection," *Journal of Heat Transfer*, Vol. 82, 1960, pp. 303–312.

[5] Papell, S. S. and Trout, A. M., "Experimental Investigation of Air Film Cooling Applied to an Adiabatic Wall by Means of an Axially Discharging Slot," TN D-9, 1959, NASA.

[6] Hartnett, J. P., Birkebak, R. C., and Eckert, E. R. G., "Velocity Distributions, Temperature Distributions, Effectiveness and Heat Transfer for Air Injected through a Tangential Slot into a Turbulent Boundary Layer," *Journal of Heat Transfer*, Vol. 83, 1961, pp. 293–306.

[7] Chin, J. H. et al., "Film Cooling with Multiple Slots and Louvers," *Journal of Heat Transfer*, Vol. 83, 1961, pp. 281–292.

[8] Eckert, E. R. G. and Birkebak, R. C., "The Effects of Slot Geometry on Film Cooling," *Heat Transfer, Thermodynamics and Education*, McGraw-Hill, New York, 1964.

[9] Dannenberg, R. E., "Helium Film Cooling on a Hemisphere at a Mach No. of 10," TN D-1550, 1962, NASA.

[10] Seban, R. A., Chan, H. W., and Scesa, S., "Heat Transfer to a Turbulent Boundary Layer Downstream of an Injection Slot," Paper 57-A-36, 1957, ASME.

[11] Seban, R. A. and Back, L. H., "Velocity and Temperature Profiles in Turbulent Boundary Layers with Tangential Injection," Paper 61-SA-24, 1962, ASME, pp. 45–54.

[12] Chin, J. et al., "Adiabatic Wall Temperature Downstream of a Single-Tangential Injection Slot," Paper 58-A-107, 1958, ASME.

[13] Goldstein, R. J. et al., "Film Cooling with Air and Helium Injection through a Rearward-Facing Slot into a Supersonic Air Flow," TR 60, Feb. 1965, Heat Transfer Lab., Univ. of Minnesota, Minneapolis, Minn.

[14] Samuel, A. E. and Joubert, P. N., "Film Cooling at an Adiabatic Flat Plate in Zero Pressure Gradient in the Presence of a Hot Mainstream and Cold Tangential Secondary Injection," contributed by Heat Transfer Division at the Winter Meeting of ASME, Dec. 1964.

[15] Gorman, R., "Shock Generators in the Hypersonic Turbulent Boundary Layer," ARL 67-0186, Sept. 1967, New York Univ., Bronx, N.Y.

[16] Bradfield, W. S., "Research on Laminar and Turbulent Boundary Layers at Supersonic Speeds," Research Report Dept. 131, Dec. 1957, Rosemount Aero Lab., Univ. of Minnesota.

[17] Eckert, E. R. G., "Survey of Heat Transfer at High Speeds," Dec. 1961, Univ. of Minnesota, Minneapolis, Minn.

[18] Zakkay, V. and Callahan, C. J., "Laminar, Transitional and Turbulent Heat Transfer to a Cone-Cylinder Flare Body at Mach 8," *Journal of the Aerospace Sciences*, Vol. 29, No. 12, Dec. 1962, pp. 1403–1413.

[19] Baronti, P. O. and Libby, P. A., "Velocity Profiles in Turbulent Compressible Boundary Layers," *AIAA Journal*, Vol. 4, No. 2, Feb. 1966, pp. 193–202.

[20] Coles, D. R., "The Turbulent Boundary Layer in a Compressible Fluid," Rept. R-403-PR, Sept. 1962, Rand Corp., Los Angeles, Calif.

[21] Spalding, D. B. and Chi, S. W., "The Drag of a Compressible Turbulent Boundary Layer on a Smooth Flat Plate with and without Heat Transfer," *Journal of Fluid Mechanics*, Jan. 1964, pp. 117–143.

[22] Seban, R. A., "Effect of Initial Boundary Layer Thickness on a Tangential Injection System," *Transaction of ASME*, Ser. C; *Journal of Heat Transfer*, Vol. 82, Nov. 1960, pp. 392–393.

[23] Kleinstein, G., "Finite Difference Solution of the Laminar Compressible Boundary Layer Equations in the von Mises Variables with Applications," ARL-67-0050, March 1967, New York Univ., New York.

[24] Goldstein, R. J., Tsou, F. K., and Eckert, E. R. G., "Film Cooling in Supersonic Flow," Rept. TR-54, Dec. 1963, Heat Transfer Lab., Univ. of Minnesota, Minneapolis, Minn.

[25] Parthasarathy, K. and Zakkay, V., "Turbulent Slot Injection Studies at Mach 6," ARL-69-0066, April 1969, New York Univ., New York.

[26] Tribus, M. and Klein, J., "Forced Convection from Non-Isothermal Surfaces," *Heat Transfer Symposium*, University of Michigan Press, Ann Arbor, 1953, pp. 211–235.

[27] Goldstein, R. J. et al., "Film Cooling with Air and Helium Injection through a Rearward-facing Slot Into a Supersonic Airflow," *AIAA Journal*, Vol. 4, No. 6, June 1966, pp. 981–985.